

Figure S1:

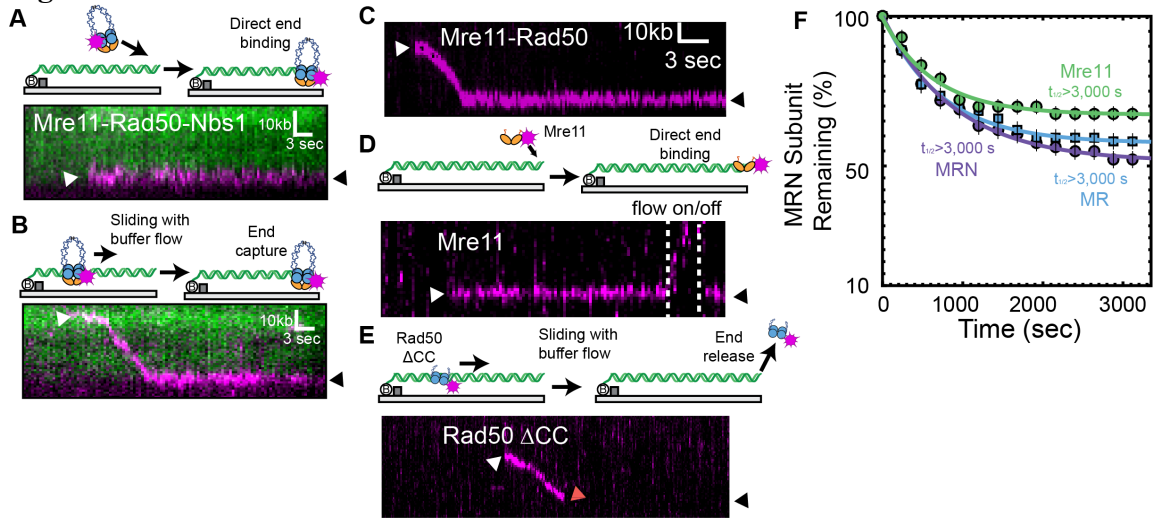


Figure S1. Characterization of individual MRN subunits on DNA curtains, Related to Figure 1.

(A) Illustration (top) and kymographs of MRN (magenta) binding to fluorescently labeled DNA (green) via 3D collision or (B) 1D sliding. (C) MR, (D) Mre11, and (E) Rad50 Δ CC interactions with DNA. White arrows indicate binding events. Red arrow: dissociation event. Black arrows mark the free DNA end. The DNA is not stained with a fluorescent dye in panels (C)-(E). To confirm that Mre11 is on a DNA end, we turned buffer flow off and on (dashed lines, middle panel). As expected for a DNA-bound molecule, Mre11 responds to buffer flow and retracts to the top DNA barrier. (F) Lifetime of MRN (purple, N = 71), MR (blue, N = 79), and Mre11 (green, N=43) on DNA with indicated half-lives ($t_{1/2}$). The half-life for Rad50 Δ CC was not determined because the protein slides off the DNA ends.

Figure S2:

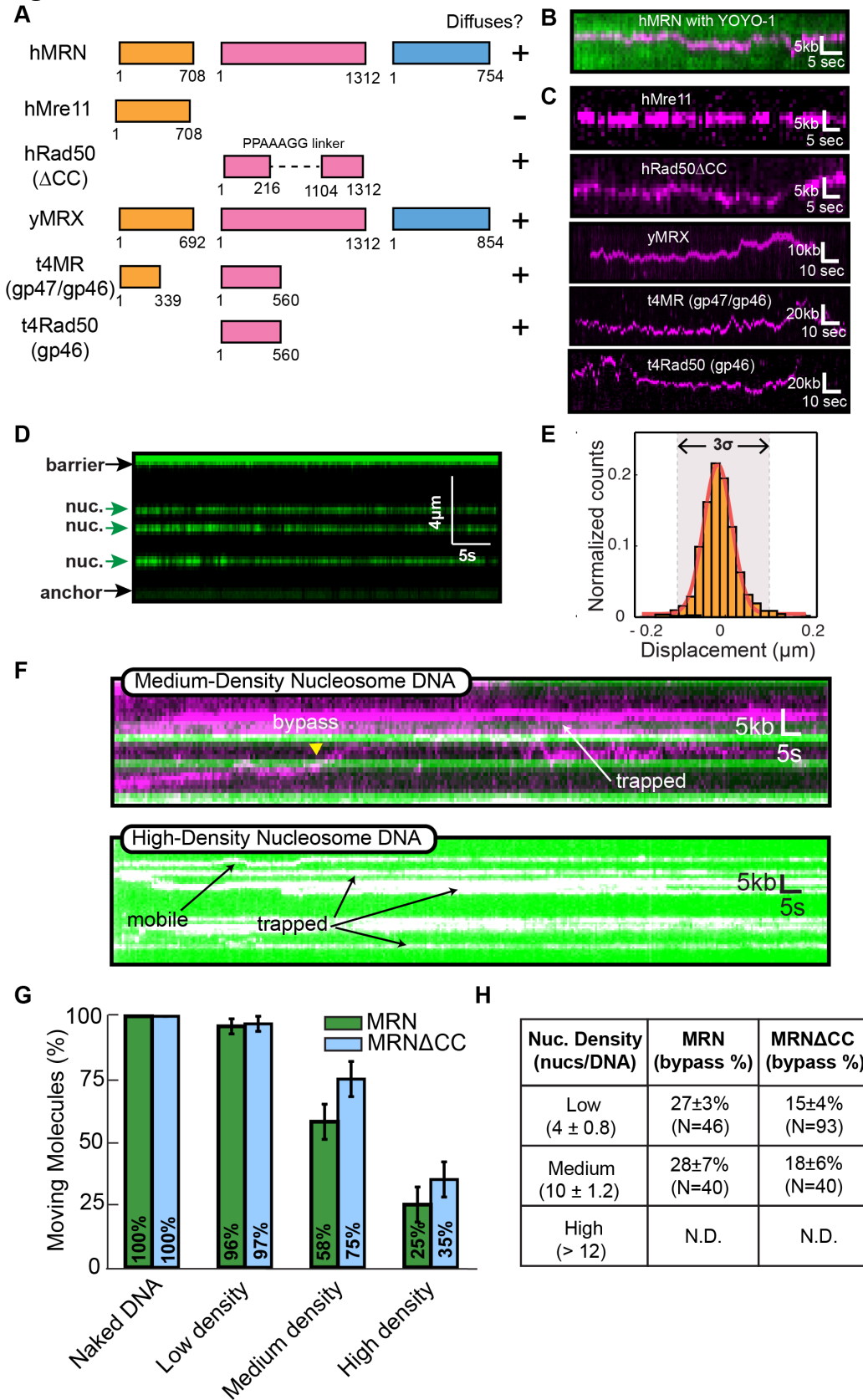


Figure S2. Characterization of MRN and variants diffusion, Related to Figure 2.

(A) Domain map of individual subunits characterized in this study: Mre11 in orange, Rad50 in pink, and Nbs1/Xrs2 in blue. (B) hMRN (magenta) diffusing on a fluorescent DNA molecule (green). (C) Representative kymographs of several sub-complexes on double-tethered DNA. hMre11 did not diffuse within our resolution. The DNA is not fluorescently labeled in panel (C). (D) Kymograph of a double-tethered DNA molecule with nucleosomes (green). Black arrows indicate fabricated DNA barriers and anchors. Green arrows: fluorescent nucleosomes. (E) Net displacement of 26 nucleosome trajectories. To define ‘nucleosome zone’ boundary, 2600 displacement values from 26 molecules were combined and fit to a Gaussian distribution. The Gaussian fit (red line) gives a center of $0.013 \pm 0.04 \mu\text{m}$ (S.D.), and 3 standard deviations ($3\sigma = 0.12 \mu\text{m}$) were used to define the nucleosome zone (gray rectangle). (F) Representative kymographs of MRN (magenta) diffusing past nucleosomes (green) on medium-density (average of 10 ± 1.2 nucleosomes/DNA; $N = 40$ DNA molecules), and high-density nucleosome DNA (>12 nucleosomes/DNA; $N = 40$ DNA molecules). Yellow arrows indicate nucleosome bypass events. (G) Quantification of moving MRN molecules on nucleosome DNA substrates. (H) Nucleosome bypass probabilities as a function of nucleosome density. Bypass probabilities could not be determined (N.D.) for high nucleosome density DNA due to optical resolution limits. S.D. in (G) and (H) obtained via bootstrapping.

Figure S3:

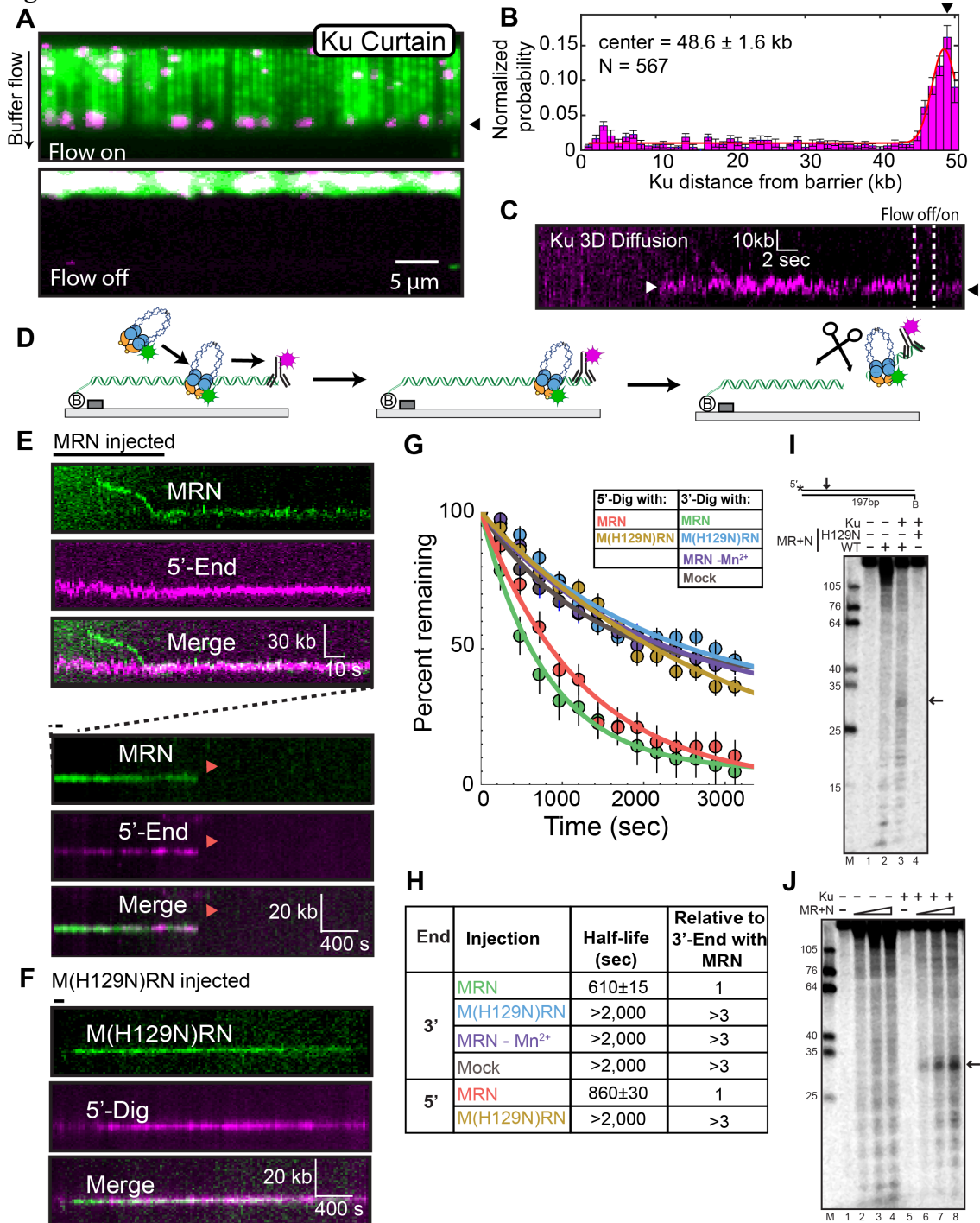


Figure S3. Single-molecule analysis of Ku70/Ku80 (Ku) and Dig end removal by MRN, Related to Figure 3.

(A) Ku (magenta) bound to DNA (green) in the presence (top) or absence (bottom) of buffer flow. Ku molecules retract to the linear DNA barrier in the absence of buffer flow (bottom). (B) Histogram of Ku binding along the DNA substrate. As expected, Ku prefers to bind free DNA ends. Error bars are the SD as determined by bootstrapping. The inset indicates the center and SD of the Gaussian fit (red line). (C) Kymograph of Ku binding a free DNA end. Dotted white lines show where buffer flow was briefly turned off and then back on. Ku retracts to the barrier when buffer flow was off, confirming that it is at the free DNA end. White arrow indicates DNA binding event. Black arrows throughout indicate the DNA end. (D) Illustration of MRN-dependent DNA end cleavage. The 3' or 5'-DNA end is fluorescently labeled with an anti-digoxigenin conjugated quantum dot (QD, magenta). MRN (green) initially binds homoduplex DNA (left). In the presence of buffer flow, MRN slides to the DNA end (middle). MRN nucleolytically removes itself and the DNA end label (right). (E) Kymograph of MRN sliding to the DNA end (top) and nucleolytically removing the fluorescent label (bottom, red arrows). (F) Kymograph as in (E) with nuclease-deficient M(H129N)RN. The fluorescent DNA label is not lost for the duration of the movie. (G) Lifetime of the 5' or 3'-labeled DNA ends in the presence of MRN, M(H129N)RN, or with MRN in the absence of Mn^{2+} . (H) Summary of the data in (G). Right column: lifetimes relative to MRN-dependent cleavage of the 3' end. (I) Nuclease assay of Ku-blocked ends with MR+N or M(H129N)R+N on a 197bp PCR substrate. MRN cleaves the DNA ~30 nt away from the radiolabeled end in a Ku and nuclease-dependent manner. As previously reported, limited MRN exonuclease activity is visible in the absence of Ku (Cannavo and Cejka, 2014). Wild-type MR or M(H129N)R (50 nM) and 50 nM Nbs1 were incubated with 5' radiolabeled 197 bp dsDNA containing 10 nM Ku in the presence of 1 mM ATP, 5 mM $MgCl_2$, 1 mM $MnCl_2$, at 37°C for 30 min. Reaction products were separated on a denaturing polyacrylamide gel and analyzed by phosphorimager. (J) Titration of MR+N on the same substrate as f with or without Ku. MRN in the presence of Ku generates a concentration-dependent and Ku-dependent ~30 nt product. hMR wild-type (12.5, 25 and 50 nM) and equimolar Nbs1 were incubated with 5'-radiolabeled 197-bp dsDNA containing 10 nM Ku in the presence of 1 mM ATP, 5 mM $MgCl_2$, and 1 mM $MnCl_2$, at 37°C for 30 min. Arrows in (I) and (J) indicate the cleavage product.

Figure S4:

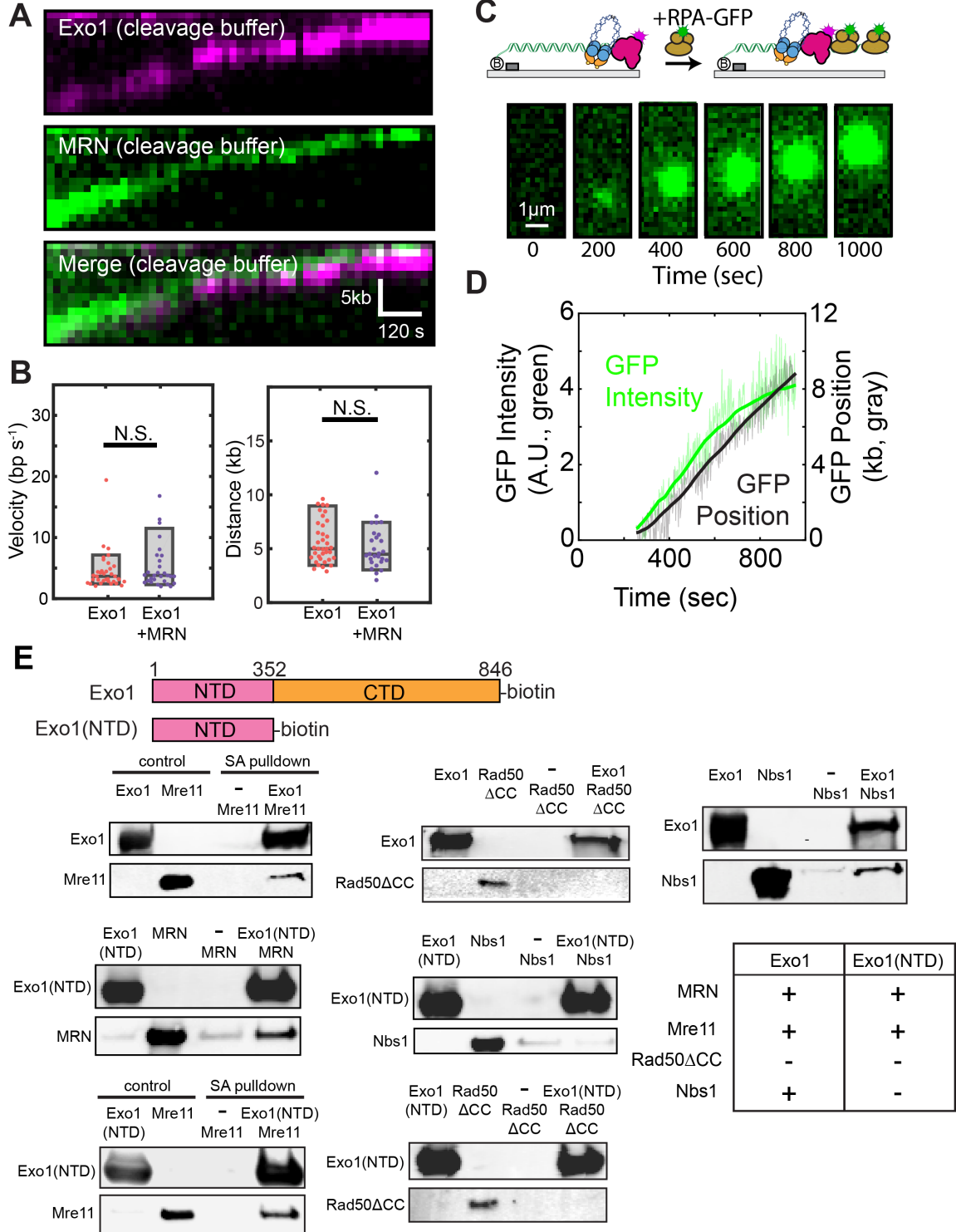


Figure S4. Characterization of Exo1 and MRN interaction, Related to Figure 4.

(A) Kymograph of Exo1 (magenta)-MRN (green) resection in MRN cleavage buffer (supplemented with Mg^{2+} , Mn^{2+} and ATP). (B) Velocity (left) and processivity (right) of Exo1 in MRN cleavage buffer in the absence (red, N=35) or presence (purple, N=27) of MRN. N.S. indicates a p-value > 0.05 (student's t-test). MRN does not stimulate Exo1 velocity and processivity. (C) MRN/Exo1 resection produces long ssDNA products. Snapshot of RPA-GFP accumulation at indicated times on a single DNA end. RPA-GFP accumulation requires both Exo1 and MRN for processive resection. (D) Quantification of the RPA-GFP intensity (green, left axis) and RPA-GFP position (black, right axis) for the molecule shown in (C). Solid lines represent a twenty-frame moving average filter of the raw particle tracking intensities (green) or positions (black). (E) Domain map of Exo1-biotin and Exo1(NTD)-biotin proteins used for pulldown assays. The catalytic NTD (pink) and largely disordered CTD (orange) of Exo1 are indicated. Streptavidin pulldown assays showing the interactions of full-length Exo1 (left) or Exo1-NTD (right) with individual MRN subunits or the full complex. Table summarizing MRN Exo1 interactions. These interactions were maintained even with stringent DNase treatment (See STAR Methods).

Table S1. MRN diffusion coefficients, Related to Figure 2.

Condition	Total ionic strength (mM)	[NaCl] (mM)	1D diffusion coefficient \pm S.E.M. ($\mu\text{m}^2 \text{s}^{-1}$)	Number of molecules	p-value (relative to 23 mM total ionic strength)
No nucleotide	23	0	0.164 ± 0.017	42	N/A
No nucleotide	53	30	0.172 ± 0.029	34	0.871
No nucleotide	83	60	0.157 ± 0.013	34	0.766
No nucleotide	143	120	0.238 ± 0.021	51	0.053
ADP	23	0	0.151 ± 0.024	38	0.754
ATP	23	0	0.123 ± 0.011	76	0.346
ATP-Mg⁺²	23	0	0.129 ± 0.014	99	0.244

Note: P-values were calculated using the Mann-Whitney test for non-parametric distributions.

Table S2. Half-life of proteins in various conditions, Related to Figure 3.

Condition	Half-life \pm 95% confidence interval (sec)	Number of molecules
Ku alone	> 3,000	80
Ku + MRN (no Mn²⁺)	> 3,000	111
Ku + MRN (no ATP)	> 3,000	100
Ku + MRN	400 \pm 6	140
Ku + MR	> 3,000	59
Ku + MR + Nbs1	480 \pm 15	50
Ku + M(H129N)RN	> 3,000	79
3' Dig Antibody	>2,000	43
3' Dig Antibody + MRN	610 \pm 15	42
3' Dig Antibody + MRN (no Mn²⁺)	>2,000	41
3' Dig Antibody + M(H129N)RN	>2,000	24
5' Dig Antibody + MRN	860 \pm 30	57
5' Dig Antibody + M(H129N)RN	>2,000	36
MRN diffusion	56 \pm 3	101
MRN diffusion + labeled nucleosomes	39 \pm 1	85
MRN diffusion + unlabeled nucleosomes	55 \pm 2	44
MRNΔCC diffusion	63 \pm 2	48
MRNΔCC diffusion + labeled nucleosomes	14 \pm 2	90
MRNΔCC diffusion + unlabeled nucleosomes	10 \pm 1	90

Table S3: Oligonucleotides used in this study, Related to STAR Methods.

Name	Sequence
IF007	[p]AGG TCG CCG CCC[Bio]
IF009	[p]GGG CGG CGA CCT[Dig]
IF075	GGTGGTGAATTCCATATGAAGAATTTTAAACTTAATAG
IF076	GGTGGTTCTAGAGCTCTTCCGCATTAACCATTACAGTAAATCG
IF077	ACAGCTTATCGGAATGTCTTATGCCAGTTTCAAGCAG
IF078	CTGCTTGAAACTGGCATAAGACATTCCGATAAGCTGT
IF079	GGTGGTCATATGAAAATTTTAAATTTAGGTG
IF080	TATGAACTCGAGTTGTGTTGCCTCTACATATA
IF115	TCTAGAGCCTGCAGTCTCGAG
IF116	GATATCCTGCATAGTCCGGGACGTCATAGGGATAGCCAGCGTAA TCTGGAACATCGTATG
IF117	CCTACGATGTGCCAGACTATGCGTAGTCTAGAGCCTGCAGTCTC G
IF183	ATTATAAAGATCATGATATCGACTACAAGGACGATGACGATAA ATAGG
IF184	[p]CACCGTCATGGTCTTTGTAGTCTGCTCCGAGTCTTCTATTTCTT CTAA
LM002	CTAAGCGTAATCTGGAACATCGTATGGGTATATCATGTCCAATA AATCGTCCACATCACC
LM003	[p]GGG CGG CGA CCT TT TT
LM031	GGG CGG CGA CCT
TP542	GGTTTTCCAGTCACGACGTTG
TP4535	AACGTCATAGACGATTACATTGCTAGGACATCTTTGCCACGTT GACCCA
TP4373	TGGGTCAACGTGGGCAAAGATGTCCTAGCAATGTAATCGTCTAT GACGTT
TP4629	[Dig]TGGGTCAACGTGGGCAAAGATGTCCTAGCAATGTAATCGTC TATGACGTT
TP4630	GGGCGGCGACCTAACGTCATAGACGATTACATTGCTAGGACATC TTTGCCACGTTGACCCA
TP5124	[Bio]TGGGTCAACGTGGGCAAAGATGTCCTAGCAATGTAATCGTC TATGACGTT
XBG001	GGCCTGAACGACATCTTCGAGG
XBG002	TCTTGAATGGGCAGGCATAGCA